

1 Status and future prospects of Lepton Universality tests 2 at LHCb

3 **Resmi PK**^{†,*}

4 *Aix Marseille Univ, CNRS/IN2P3, CPPM*

5 *163 avenue de Luminy, Case 902 13288 Marseille cedex 09, France*

6 *E-mail: resmi.pk@cern.ch*

7 The Standard Model is lepton flavour universal *i.e.* the couplings of electroweak gauge bosons and the different lepton families are universal. However, recent measurements have shown deviations from this behavior, which could potentially be due to contribution from new physics. The lepton flavour universality tests done at the LHCb experiment using tree-level and rare B decays are presented.

*** *The 22nd International Workshop on Neutrinos from Accelerators (NuFact2021)* ***

*** *6–11 Sep 2021* ***

*** *Cagliari, Italy* ***

[†]on behalf of LHCb Collaboration.

*Speaker

1. Introduction

The Standard Model (SM) is Lepton Flavour Universal (LFU), *i.e.* the electroweak couplings to the three charged leptons are independent of the flavour. Any difference in the way they interact is driven only by the different lepton mass. LFU has been tested extensively with measurements of ratios of branching fractions of decays involving different leptons [1]. In $b \rightarrow c\ell\nu_\ell$ transitions, the ratio $R(X_c) = \frac{\mathcal{B}(X_b \rightarrow X_c \tau^+ \nu_\tau)}{\mathcal{B}(X_b \rightarrow X_c \ell^+ \nu_\ell)}$ is measured, where X_b (X_c) is a hadron containing b (c) quark and $\ell = e, \mu$. The ratios $R_{K^*} = \frac{\mathcal{B}(B^0 \rightarrow K^{*0} \mu^+ \mu^-)}{\mathcal{B}(B^0 \rightarrow K^{*0} e^+ e^-)}$ and $R_K = \frac{\mathcal{B}(B^+ \rightarrow K^+ \mu^+ \mu^-)}{\mathcal{B}(B^+ \rightarrow K^+ e^+ e^-)}$ are measured in $b \rightarrow s\ell\ell$ transitions. The LFU test measurements performed at LHCb are presented here.

2. $b \rightarrow c\ell\nu_\ell$ decays

The tree-level semileptonic decays involving $b \rightarrow c\ell\nu_\ell$ quark transitions provide a number of possible $R(X_c)$ measurements, which are sensitive to enhanced coupling to third generation predicted by new physics models, e.g. leptoquarks [2]. The uncertainties related to form factors mostly cancel in the ratio.

Three LHCb measurements are available, all using Run 1 data collected during 2011–2012 corresponding to an integrated luminosity of 3 fb^{-1} : $R(D^*)$ and $R(J/\psi)$ measurements with muonic τ decays ($\tau^- \rightarrow \mu^- \nu_\mu \nu_\tau$) and $R(D^*)$ measurement with three-prong hadronic τ decays ($\tau^- \rightarrow \pi^+ \pi^- \pi^- (\pi^0) \nu_\tau$). Neutrinos are not reconstructed for any of the decays and specific approximations are used to reconstruct the B candidates.

2.1 Measurements with muonic τ decays

The ratio $R(D^*) = \frac{\mathcal{B}(B \rightarrow D^* \tau \nu)}{\mathcal{B}(B \rightarrow D^* \mu \nu)}$ is measured with the muonic τ decays [3]. The B candidate reconstruction is carried out with the approximation that the z -component of the B momentum is the same as that of the $D^* \mu$ system. The visible final state in both the decay modes, in the numerator and denominator of $R(D^*)$, is the same. The τ and μ decay modes are separated via a three-dimensional binned template fit to the variables $q^2 = (p_B - p_{D^*})^2$, $m_{\text{miss}}^2 = (p_B - p_{D^*} - p_\ell)^2$ and energy of the muon, where p is the momentum of the corresponding particles.

A boosted decision tree (BDT) is used to reject backgrounds with additional charged tracks. The final selected sample contains backgrounds of the types, $B \rightarrow D^{**} \mu \nu$, $B \rightarrow D^{**} \tau \nu$, $B_s \rightarrow D_s \mu \nu$, $B \rightarrow D^{**} H_c X$, where H_c decays semileptonically, random final state combinations, and hadrons (π, K, p) misidentified as muons. The templates representing probability density functions for the signal and background components are extracted from control samples and simulations that are validated against data. The fit extracts the relative contributions of signal and normalization modes along with their form factors. The fit projections are shown in Fig. 1. The result obtained, $R(D^*) = 0.336 \pm 0.027(\text{stat}) \pm 0.030(\text{syst})$, is 2.1σ above the SM prediction. The dominant systematic uncertainty comes from the limited size of the simulation sample.

The ratio $R(J/\psi) = \frac{\mathcal{B}(B_c^+ \rightarrow J/\psi \tau^+ \nu_\tau)}{\mathcal{B}(B_c^+ \rightarrow J/\psi \mu^+ \nu_\mu)}$ is also measured using the muonic decays of τ [4]. The main background in the sample comes from $B_c \rightarrow H_c X$ decays where hadron H_c is misidentified as μ . Signal is extracted using a binned template fit to m_{miss}^2 , B_c decay time and Z , where Z contains 8 bins in E_μ and q^2 (first 4 bins with $q^2 < 7.14 \text{ GeV}^2$, the rest $q^2 > 7.14 \text{ GeV}^2$). The fit results

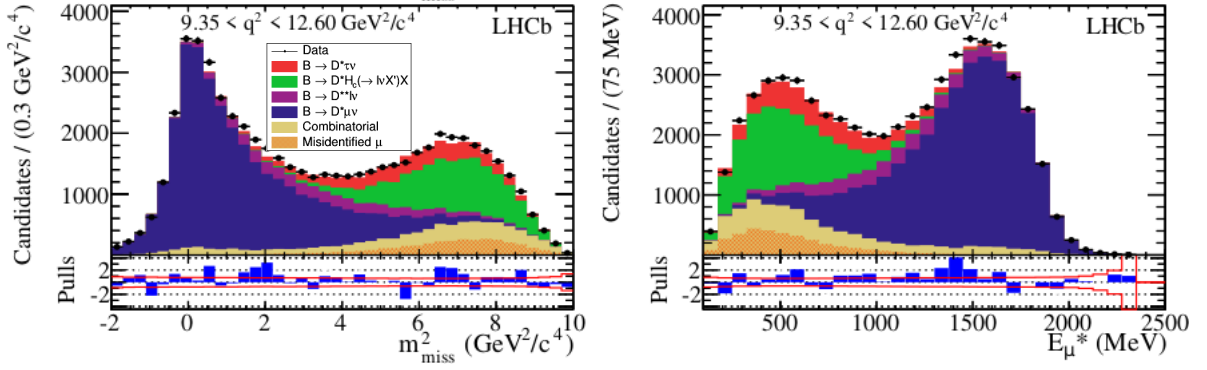


Figure 1: Distributions of m_{miss}^2 (left) and E_{μ^*} (right) in the specified q^2 bins of the signal data, overlaid with projections of the fit model with all normalization and shape parameters at their best-fit values.

46 are given in Fig. 2. This is the first evidence of the $B_c^+ \rightarrow J/\psi \tau^+ \nu_\tau$ decay mode. The $R(J/\psi)$ value
 47 obtained is $0.71 \pm 0.17(\text{stat}) \pm 0.18(\text{syst})$, which is 2σ above the predicted value from SM.

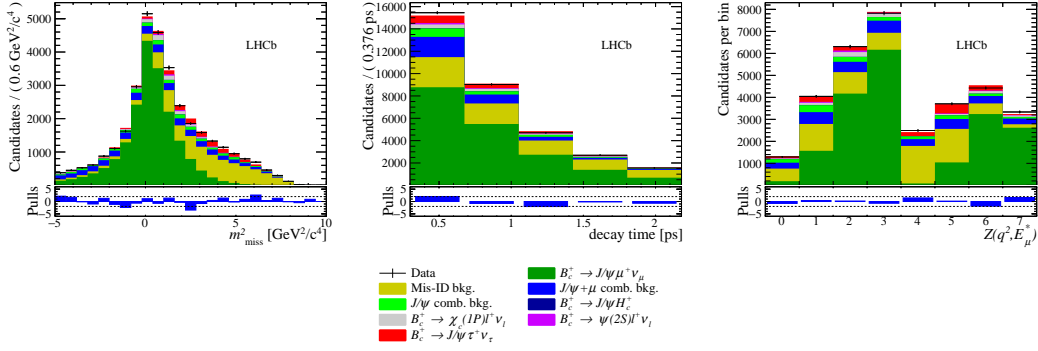


Figure 2: Distributions of m_{miss}^2 (left), decay time (middle) and Z (right) of the signal data, overlaid with projections of the fit model with all normalization and shape parameters at their best-fit values.

48 2.2 Measurements with hadronic τ decays

49 $R(D^*)$ with three-prong hadronic τ decays is measured as $R(D^*) = \mathcal{K}(D^*) \frac{\mathcal{B}(B^0 \rightarrow D^{*-} 3\pi^\pm)}{\mathcal{B}(B^0 \rightarrow D^{*-} \ell \nu_\ell)}$,
 50 where $\mathcal{K}(D^*) = \frac{\mathcal{B}(B^0 \rightarrow D^{*-} \tau^+ \nu_\tau)}{\mathcal{B}(B^0 \rightarrow D^{*-} 3\pi^\pm)}$ has been measured and the other branching fractions form external
 51 input [5]. The normalisation mode, $B^0 \rightarrow D^{*-} 3\pi^\pm$, has the same visible final state as that of the
 52 signal mode. The τ decay vertex is reconstructed from the three charged pion daughter candidates.
 53 The major backgrounds include $B \rightarrow D^{*-} 3\pi^\pm X$ prompt decays and $B \rightarrow D^{*-} (D_s^+, D^+, D^0) X$
 54 double-charm decays. The prompt decays are suppressed by requiring that the $3\pi^\pm$ vertex is
 55 displaced with respect to that of the B . The double charm backgrounds mimic the signal topology
 56 due to the non-negligible life time of the charm mesons and a BDT is deployed to suppress such
 57 events.

58 A three-dimensional binned template fit is used to extract the signal yield, with the variables
 59 $q^2 = (p_{B^0} - p_{D^*})^2$, τ^+ decay time, and the output of BDT trained to discriminate τ from D_s^+ . The fit

60 projections are shown in Fig. 3. The result, $R(D^*) = 0.280 \pm 0.018(\text{stat}) \pm 0.026(\text{syst}) \pm 0.013(\text{ext})$,
 61 is 1σ above the expected value from SM.

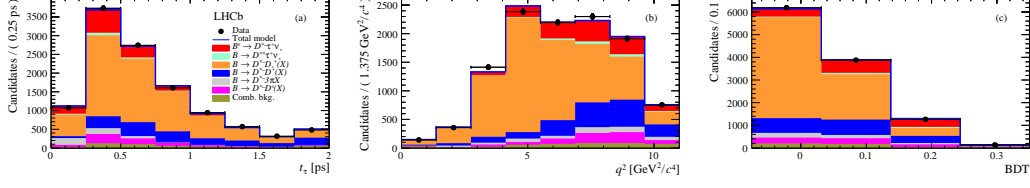


Figure 3: Distributions of τ decay time (left), q^2 (middle) and BDT output (right) of the signal data, overlaid with projections of the fit model with all normalization and shape parameters at their best-fit values.

62 There are deviations between the existing measurements and the SM expectations. In particular,
 63 the combination of $R(D)$ and $R(D^*)$ measurements is more than 3σ away from the predictions
 64 in the SM [1]. Therefore it is imperative to improve the measurements by adding more data and
 65 devise strategies to reduce dominant systematic uncertainties. More $R(X_c)$ measurements are being
 66 performed at LHCb. Furthermore, new observables beyond the branching fraction ratios are being
 67 explored to study the nature of potential new physics.

68 3. $b \rightarrow s\ell\ell$ decays

69 Flavour changing neutral current transitions such as $b \rightarrow s\ell\ell$ are suppressed in the SM
 70 making them a powerful probe for new physics. Several tensions with the SM predictions are seen
 71 in branching fractions and angular observables in these rare decays [6]. The largest theoretical
 72 uncertainties contribution are hadronic effects. However, such uncertainties mostly cancel out
 73 in ratios of branching fractions, so that they are precisely predicted, $R_H = \frac{\mathcal{B}(H_B \rightarrow H\mu^+\mu^-)}{\mathcal{B}(H_B \rightarrow He^+e^-)} =$
 74 1.00 ± 0.01 [7].

75 The double ratios $R_{K^{(*)}} = \frac{\mathcal{B}(B \rightarrow K^{(*)}\mu^+\mu^-)}{\mathcal{B}(B \rightarrow K^{(*)}e^+e^-)} \bigg/ \frac{\mathcal{B}(B \rightarrow J/\psi(\mu^+\mu^-)K^{(*)})}{\mathcal{B}(B \rightarrow J/\psi(e^+e^-)K^{(*)})}$ are measured at LHCb to gain
 76 better control of the efficiency with the help of the control mode ($B \rightarrow J/\psi K^{(*)}$) that is expected
 77 to be lepton universal even in the presence of new physics. This ensures the cancellation of most
 78 of the experimental systematic contributions to the measurements. The q^2 regions contain J/ψ and
 79 $\psi(2S)$ resonances allowing for control studies, where q^2 is the dilepton invariant mass-squared.
 80 The measurements are done in the non-resonant region, $1.1 < q^2 < 6.0 \text{ GeV}^2$.

81 The presence of electrons in the final state poses more challenges in the reconstruction at
 82 LHCb. Since they are light in mass, they interact with the detector material through bremsstrahlung
 83 emission, leading to a poorer momentum resolution compared to any other charged particles. This
 84 energy loss is recovered in the reconstruction with a non negligible inefficiency by adding to the
 85 electron momentum, the photon cluster energy in the calorimeter that is compatible with the electron
 86 direction, improving the kinematic description of electrons.

87 The latest measurement of the ratio R_K is based on the full LHCb dataset corresponding to an
 88 integrated luminosity of 9 fb^{-1} [8]. A simultaneous maximum likelihood fit to the invariant mass
 89 for the modes $B^+ \rightarrow K^+e^+e^-$ and $B^+ \rightarrow K^+\mu^+\mu^-$ is used to extract R_K . The fit projections are
 90 given in Fig. 4. The measured R_K value in $1.1 < q^2 < 6.0 \text{ GeV}^2/c^4$ is $0.846^{+0.042}_{-0.039}(\text{stat})^{+0.013}_{-0.012}(\text{syst})$

91 representing a 3.1σ evidence for the violation of LFU. The goodness of the efficiency estimation is
 92 verified using the control region of J/ψ where no cancellation of systematic effects is possible, and
 93 the portability of corrections in other q^2 regions is verified testing the double ratio with the $\Psi(2S)$
 94 mode, verifying the compatibility of $r_{(J/\psi)}$ ¹ and $R_{\Psi(2S)}$ with unity.

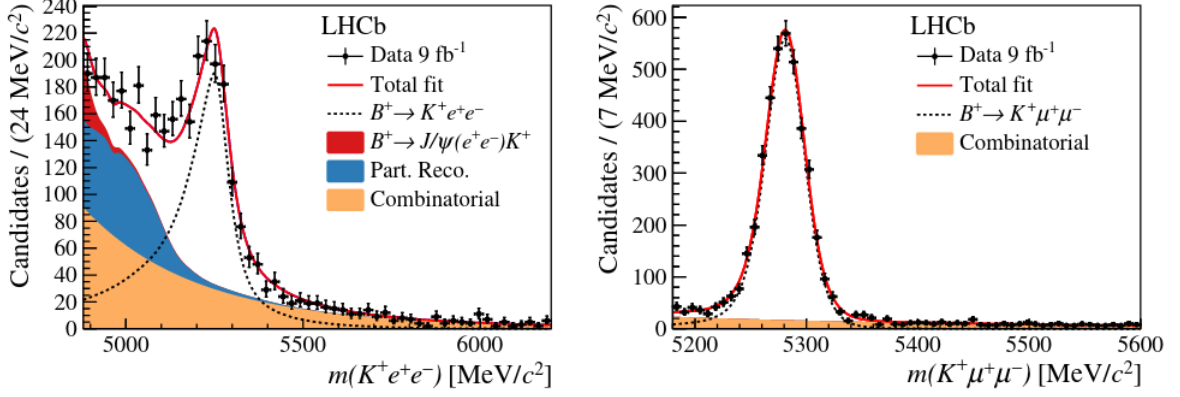


Figure 4: Distributions of $m(K^+e^+e^-)$ (left) and $m(K^+\mu^+\mu^-)$ (right) for the non-resonant signal channel. The fit projections are superimposed.

95 The other ratio measurements from LHCb include R_{K^*} from $B^0 \rightarrow K^{*0}\ell^+\ell^-$ decays with the
 96 Run 1 data [9] and R_{pK} from $\Lambda_b \rightarrow pK\ell^+\ell^-$ decays [10]. There are tensions up to 2.5σ with the
 97 SM predictions in the former, whereas the latter is compatible with the SM prediction.

98 4. Summary and prospects

99 There are several tensions with the SM predictions observed in the behaviour of leptons in B
 100 decays. There are tensions up to 3σ found in measurements involving $b \rightarrow c\ell\nu_\ell$ decays. Evidence
 101 of LFU violation is observed in $b \rightarrow s\ell\ell$ decays at the level of 3.1σ . New measurements and
 102 observables are needed to understand the nature of these discrepancies and identify the possible
 103 sources of new physics, if any. The Run 3 data taking at LHCb will start very soon during which
 104 the LHCb detector is expected to collect data corresponding to an integrated luminosity of 25 fb^{-1} .
 105 Also thanks to improved trigger and reconstruction techniques, this will allow to make more precise
 106 measurements and to explore many new observables, thus helping to further understand the nature
 107 of leptons within the SM and beyond.

108 References

- 109 [1] Y. Amhis *et al.* (Heavy Flavour Averaging Group), Eur. Phys. J. **C81** 226 (2021).
 110 [2] A. Crivellin, J. Heeck, and P. Stoffer, Phys. Rev. Lett. **116**, 081801 (2016).
 111 [3] R. Aaij *et al.* (LHCb Collaboration), Phys. Rev. Lett. **115**, 111803 (2015).

¹ $r_{J/\psi} = \frac{\mathcal{B}B^+ \rightarrow J/\psi(\rightarrow \mu^+\mu^-)K^+}{\mathcal{B}B^+ \rightarrow J/\psi(\rightarrow e^+e^-)K^+}$

- 112 [4] R. Aaij *et al.* (LHCb Collaboration), Phys. Rev. Lett. **120**, 121801 (2018).
113 [5] R. Aaij *et al.* (LHCb Collaboration), Phys. Rev. Lett. **120**, 171802 (2018).
114 [6] R. Aaij *et al.* (LHCb Collaboration), Phys. Rev. Lett. **126**, 161802 (2021).
115 [7] S. Descotes-Genon, L. Hofer, J. Matias, and J. Virto J. High Energ. Phys. **2016** 92 (2016).
116 [8] R. Aaij *et al.* (LHCb Collaboration), arXiv:2103.11769v1.
117 [9] R. Aaij *et al.* (LHCb Collaboration), J. High Energ. Phys. **2017**, 55 (2017).
118 [10] R. Aaij *et al.* (LHCb Collaboration), J. High Energ. Phys. **2020**, 40 (2020).